J Appl Physiol 112: 824–831, 2012.
First published October 27, 2011; doi:10.1152/japplphysiol.00975.2010.

Jamming dynamics of stretch-induced surfactant release by alveolar type II cells

Arnab Majumdar, Stephen P. Arold, Erzsébet Bartolák-Suki, Harikrishnan Parameswaran, and Béla Suki
Department of Biomedical Engineering, Boston University, Boston, Massachusetts

Submitted 23 August 2010; accepted in final form 24 October 2011

Majumdar A, Arold SP, Bartolák-Suki E, Parameswaran H, Suki B. Jamming dynamics of stretch-induced surfactant release by alveolar type II cells. *J Appl Physiol* 112: 824–831, 2012. First published October 27, 2011; doi:10.1152/japplphysiol.00975.2010.— Secretion of pulmonary surfactant by alveolar epithelial type II cells is vital for the reduction of interfacial surface tension, thus preventing lung collapse. To study secretion dynamics, rat alveolar epithelial type II cells were cultured on elastic membranes and cyclically stretched. The amounts of phosphatidylcholine, the primary lipid component of surfactant, inside and outside the cells, were measured using radiolabeled choline. During and immediately after stretch, cells secreted less surfactant than unstretched cells; however, stretched cells secreted significantly more surfactant than unstretched cells after an extended lag period. We developed a model based on the hypothesis that stretching leads to jamming of surfactant traffic escaping the cell, similar to vehicular traffic jams. In the model, stretch increases surfactant transport from the interior to the exterior of the cell. This transport is mediated by a surface layer with a finite capacity due to the limited number of fusion pores through which secretion occurs. When the amount of surfactant in the surface layer approaches this capacity, interference among lamellar bodies carrying surfactant reduces the rate of secretion, effectively creating a jam. When the stretch stops, the jam takes an extended time to clear, and subsequently the amount of secreted surfactant increases. We solved the model analytically and show that its dynamics are consistent with experimental observations, implying that surfactant secretion is a fundamentally nonlinear process with memory representing collective behavior at the level of single cells. Our results thus highlight the importance of a jamming dynamics in stretch-induced cellular secretory processes.

mathematical model; fusion pore; secretion

SECRETION OF VARIOUS MOLECULES by cells is a fundamental process of life that helps maintain an appropriate cellular microenvironment (6, 22). In the lung, the secretion of surfactant, a complex lipid-protein mixture, by alveolar epithelial type II (AEII) cells plays a pivotal role in enabling gas exchange by lowering the surface tension at the air-liquid interface (5, 10). The secretion of pulmonary surfactant has been found to be a slow stochastic process that involves packing the constituent lipids and proteins into lamellar bodies (LBs) and releasing the LB content into the extracellular space through fusion pores (9, 15). Among the many secretory stimulants, mechanical stretching of AEII cells appears to be the most potent (12, 27). However, little is known about the stretch-induced temporal dynamics of surfactant secretion and the associated mechanisms.

In this study, we present experimental evidence that, contrary to the current view, certain stretch patterns are temporarily inhibitory and delay the secretion of surfactant. To interpret these results, we developed a simple model of stretch-induced secretion based on the hypothesis that excessive stretch leads to jamming of activated LBs trying to escape the cell through a limited number of fusion pores. We solved the model analytically and show that its dynamics are in agreement with the experimental observations.

Address for reprint requests and other correspondence: B. Suki, Dept. of Biomedical Engineering, Boston Univ., 44 Cummington St., Boston, MA 02215 (e-mail: bsuki@bu.edu).

METHODS

Experiments. The protocol was approved by the Institutional Animal Care and Use Committee at Boston University. AEII cells were isolated from Sprague-Dawley rats using a technique adapted from Dobbs et al. (11). The details of the protocol are described in detail by Arold et al. (3). Briefly, the rats were anesthetized, and the pulmonary artery was perfused to remove blood. The lungs were then excised and lavaged with phosphate-buffered saline and digested with 8 ml elastase solution (5 U/ml, Sigma, St. Louis, MO) for 30 min. Following digestion, the lungs were finely minced and filtered. The resulting supernatant was incubated for 1 h on Petri dishes coated with immunoglobulin G (Sigma) for differential adhesion. The nonadherent cells were removed and centrifuged, then resuspended in media, and seeded at 10^6 cells/cm^2 on bioflex elastic membranes (Flexcell International, Hillsborough, NC) precoated with 50 μg/ml human fibronectin (Roche Diagnostics) for 24 h. Cell seeding was limited to a circular area of 0.9 cm^2 in the center of the membrane. The yield of AEII cells was in the range of $30–40 \times 10^6$ cells per rat, with >95% purity per isolation.

The seeded cells were immediately incubated in the presence of radioactive ^{3}H-labeled choline (1 μCi/ml) to label phosphatidylcholine (PC), the primary lipid constituent of pulmonary surfactant. Following incubation, the elastic membranes were placed directly above cylindrical indenter posts, and the membranes were vertically displaced by a computer-controlled linear actuator (4). The downward pulling of each membrane over the indenter post resulted in radial, as well as circumferential, expansion of the elastic membrane, causing the membrane and hence the adhered cells to receive equi-biaxial changes in surface area.

The cell populations were divided into several groups. The first group was left unstretched and served as the control group with baseline secretion. The remaining groups were cyclically stretched at a rate of 3 cycles/min with an amplitude of 50% change in surface area for stretch periods T of 15, 30, or 60 min. Samples were collected immediately at the end of the stretch period, as well as at subsequent times up to 60 min. For example, the cell populations that received 15 min of stretch were divided into three subgroups in which the samples were collected at 15, 30, or 60 min. This allowed us to track the effect of stretch on secretion after the stretch stopped. At the designated time points, the media was removed, the cells were lifted, and the lipids from both the media and the cells were isolated using the Folch partitioning (4). The percent ^{3}H-labeled PC secretion was defined as the radioactive counts per minute of the media normalized by the total detections per minute of the cells and media averaged over six samples.

To make sure that the surfactant detected in the media was a result of secretion rather than due to cell membrane injury caused by stretching, the live and dead or injured cells were fluorescently labeled for each stretch condition using three additional groups. The three groups of cells were stretched for 15, 30, or 60 min, and the live/dead assay was carried out at 60 in each group. Cells were first incubated in the presence of ethidium homodimer-1 and calcein AM. Ethidium homodimer-1 only enters cells with a compromised plasma membrane

and fluoresces bright red, whereas calcein AM fluoresces bright green within live cells. After labeling, the cells were examined using an upright fluorescent microscope, and images were captured from five random locations in each well. The fractions of dead and/or injured cells were calculated as the ratio of dead and injured cells to the total number of cells. The total count of live and dead cells showed no significant difference between groups, indicating that there was little cell detachment as in the previous study (3).

To determine whether stretch had any effect on surfactant uptake, unlabeled cells were placed in serum-free DMEM containing 1 μCi/ml ^{3}H-labeled PC (3). The cells were then stretched according to the prescribed protocol. Following the 1-h treatment period, the cells underwent the Folch partition. The uptake was calculated as the ratio of detections per minute in the stretched cells, normalized to the detections per minute in unstretched control cells.

RESULTS

Experiments. Part of the experimental data was reported earlier (2). An example of cells adhered to the membrane containing LBs is shown in Fig. 1. Figure 2 shows the fraction of surfactant secreted by the AEII cells for different stretching times *T*. At 15 min, cells undergoing stretch secreted significantly less (one-way ANOVA, $P < 0.05$) surfactant compared with unstretched cells (circles in Fig. 2). This indicates that the stretch pattern inhibited surfactant secretion at this time point. Similarly, at 30 min, all cell populations that experienced stretch secreted less surfactant than the unstretched cells; however, this decrease was not statistically significant. The secretion by cells that were stretched for the first 15 min and were unstretched for the next 15 min (squares in Fig. 2) was indistinguishable from cells that were stretched for the entire 30 min. At 60 min, cells that only experienced 15 min of stretch demonstrated a remarkable increase in secretion, surpassing the amount secreted by the unstretched cells (one-way ANOVA, $P < 0.05$). However, the cells that experienced longer durations of stretch (diamonds and triangles in Fig. 2) continued to secrete less than the unstretched cells (one-way ANOVA, $P < 0.05$).

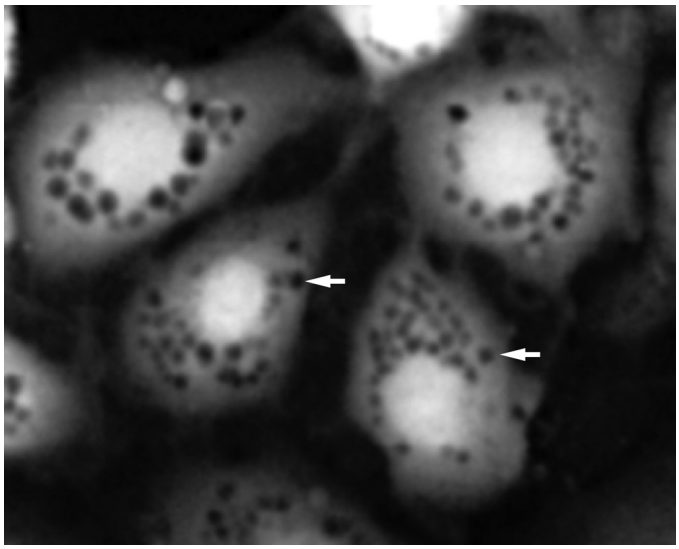

Fig. 1. Unstretched alveolar epithelial type II cells isolated from rats and imaged using an upright fluorescent microscope (Nikon Eclipse 80i). The dark spots inside the cells, indicated by arrows, show lamellar bodies containing surfactant.

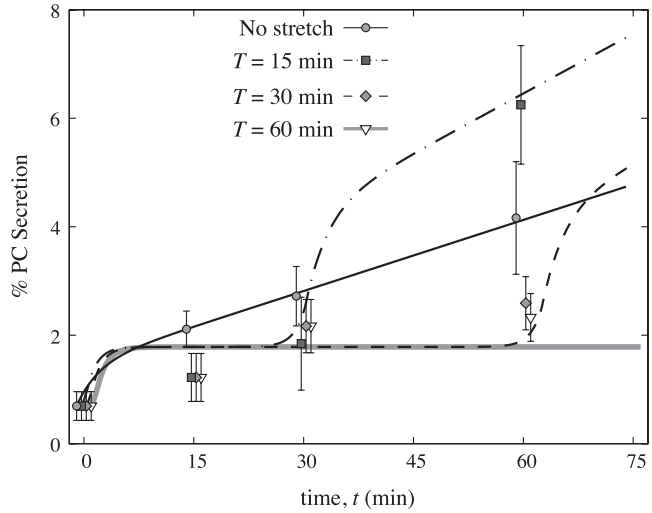

Fig. 2. Percent ^{3}H-labeled phosphatidylcholine (PC) secretion from experiments (symbols) and model fits (lines) corresponding to control (circles, thin solid line) and stretch periods *T* of 15 min (squares, dash-dotted line), 30 min (diamonds, dashed line), and 60 min (triangles, thick gray line). The error bars represent standard deviation, and each data set corresponds to $n = 6$ samples. The model parameters are as follows: $\lambda^{-1} = 3$ min, $m_0 = 0.59\ m_P$, $M = 1.46\ m_P$, $\phi_0 = 0.09\ Q_{max}$, and $\Phi = 2.01\ Q_{max}$. The experimental background of 0.7% is added to the model results. The data and model fits are both horizontally shifted for clarity. See text for definition of terms used in figure legends.

The percent dead cells showed no difference, indicating that these observations were not a result of cell death or injury (Table 1). Stretch for any duration had no significant effect on surfactant uptake, suggesting that surfactant re-uptake by AEII cells did not play a significant role in the mechanism of stretch-induced PC secretion (Table 2).

Model. Our model is based on the hypothesis that, when the cells are sufficiently stimulated by stretch, the surfactant traffic from the inside of the cell to the extracellular environment can become jammed. The model consists of a large number of identical cells adhered to an elastic membrane. The secretion of LBs in a typical cell involves a two-step process demonstrated schematically in Fig. 3*A*. We assume that a large pool of surfactant is available inside the cells separated from the outside by a membrane, or surface layer, which can store LBs. The surfactant inside the cells is continually packaged into LBs and driven up to the surface layer, resulting in an LB transport with current $\phi(t)$, which is a function of the instantaneous stretch experienced by the cells at time *t*. In the absence of stretch, the cells maintain a constant baseline current ϕ_0. At any given time, the surface layer contains a number of LBs of total mass m_S waiting to be secreted. The outflow current Q from the surface to the extracellular space is a function of m_S, similar to the fundamental diagram in the dynamics of vehicular traffic (7, 21). We define m_P as a threshold value of m_S,

Table 1. *Mean percent dead cells (along with SD) following stretch of time T and assaying at 60 min*

Stretch Time *T*, min	Dead Cells, %
15	2.41 ± 1.25
30	2.90 ± 1.28
60	2.69 ± 1.88

Values are means ± SD.

Table 2. *Mean phosphatidylcholine absorption (along with SD) normalized to control cells for different stretch durations T*

Stretch Time T, min	Uptake, %
0	1.00 ± 0.52
15	0.72 ± 0.50
30	0.49 ± 0.23
60	0.72 ± 0.28

Values are means ± SD; $n = 6$ for each point.

beyond which jamming occurs in the outflow process. For $m_S < m_P$, Q increases with m_S up to a maximum outflow $Q = Q_{max}$, when $m_S = m_P$. For $m_S > m_P$, we assume that the LBs at the surface begin to exhibit jamming, and Q decreases as m_S increases until $Q = 0$ at $m_S = M$, the maximum capacity of the surface. For simplicity, we assume that the function $Q(m_S)$ to be piecewise linear, as shown in Fig. 3*B*, allowing an analytic treatment of the model. Thus,

$$Q(m_S) = Q_{max} \times \begin{cases} \dfrac{m_S}{m_P} & \text{if } m_S \le m_P \\ \dfrac{M - m_S}{M - m_P} & \text{if } m_S > m_P \end{cases} \quad (1)$$

Note that the finite mass m_S of surfactant retained at the surface provides the system with memory.

In addition to jamming in $Q(m_S)$, we assume that, when $m_S > m_P$, the overloaded surface reflects part of $\phi(t)$, which we model as a backflow current $\phi_b(m_S, t)$, such that

$$\phi_b = \phi(t) \times \begin{cases} 0 & \text{if } m_S \le m_P \\ \dfrac{m_S - m_P}{M - m_P} & \text{if } m_S > m_P \end{cases} \quad (2)$$

This ensures that m_S never exceeds M, since as $m_S \to M$ the net inflow to the surface $\phi(t) - \phi_b(m_S, t) \to 0$, as well as the net outflow $Q(m_S) \to 0$.

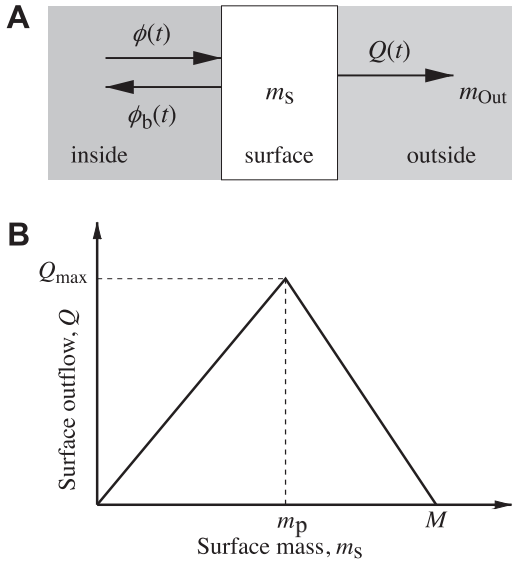

Fig. 3. Block diagram of the model of surfactant secretion (*A*), and the fundamental diagram $Q(m_S)$ of the surface corresponding to the model (*B*).

The differential equations that govern the dynamics of m_S and m_{Out}, the mass of surfactant outside the cell, are

$$\frac{dm_S}{dt} = \phi(t) - \phi_b(m_S, t) - Q(m_S) \quad (3a)$$

$$\frac{dm_{Out}}{dt} = Q(m_S) \quad (3b)$$

as illustrated in Fig. 3*A*. As in the experiments, at $t = 0$, the mass at the surface $m_S(0) = m_0 < m_P$ and the mass outside $m_{Out}(0) = 0$. Cells are then stretched for time T, such that $\phi(t) = \Phi$ for $t < T$, and $\phi(t) = \phi_0$ for $t > T$ when stretching ceases.

In the absence of stretch, $\phi(t) = \phi_0 < Q_{max}$, and we assume that no jamming occurs, $m_S(t) < m_P$. Thus the solutions to *Eqs. 1–3* are given by

$$m_S(t) = \left(m_0 - \frac{\phi_0}{\lambda}\right)e^{-\lambda t} + \frac{\phi_0}{\lambda} \quad (4a)$$

$$m_{Out}(t) = m_0 - m_S(t) + \phi_0 t \quad (4b)$$

where $\lambda = Q_{max}/m_P$. The thin solid lines in Fig. 4 show plots of $m_S(t)$ and $m_{Out}(t)$, respectively. Note that $1/\lambda$ provides a

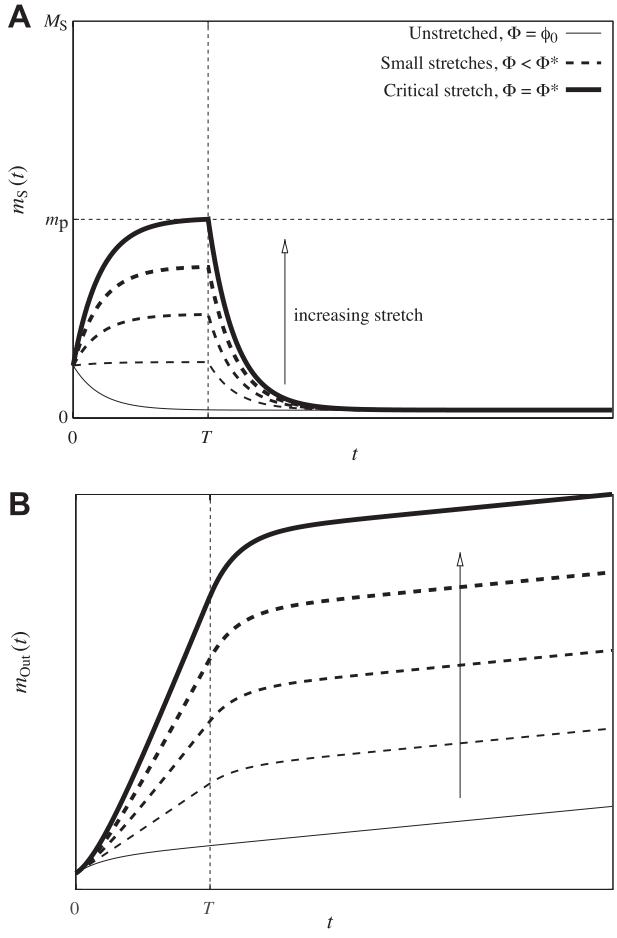

Fig. 4. Model results for the mass of surfactant in arbitrary units at the surface $m_S(t)$ (*A*) and in the extracellular space $m_{Out}(t)$ (*B*) for *1*) no stretch, $\Phi = \phi_0$, described by *Eq. 4*, shown as thin solid lines; *2*) small stretches that do not cause jamming, $\Phi < \Phi^*$, described by *Eq. 6*, shown as dashed lines; and *3*) critical stretch, which initiates jamming, $\Phi = \Phi^*$, shown as thick solid line. Arrows indicate increasing Φ.

natural time constant for this system. For $t >> 1/\lambda$, the surfactant content of the surface approaches a constant $m_S \rightarrow \phi_0/\lambda$, while the mass of secreted surfactant increases linearly, $m_{Out} \rightarrow (m_0 - \phi_0/\lambda) + \phi_0 t$.

When the cells are cyclically stretched, we assume that the time period of stretch is much smaller than the system time constant $1/\lambda$, and thus $\phi(t)$ can be approximated to have a constant value Φ during the time of stretch T. We mimic the experimental protocol by setting $\phi(t) = \Phi$, corresponding to stretching, for $0 < t \leq T$ followed by $\phi(t) = \phi_0$, corresponding to no stretching, for $t > T$,

$$\phi(t) = \begin{cases} \Phi & \text{for } t \leq T \\ \phi_0 & \text{for } t > T \end{cases} \quad (5)$$

We define Φ^* as the stretched activation rate beyond which jamming occurs after stretching for $t = T$. Thus, for $\Phi < \Phi^*$, there is no jamming and *Eq. 3* can be solved for $m_S(t)$ and $m_{Out}(t)$ yielding,

$$m_S(t) = \left(m_0 - \frac{\Phi}{\lambda}\right)e^{\lambda t} + \frac{1}{\lambda}\begin{cases} \Phi & \text{for } t \leq T \\ \phi_0 + \Delta\Phi e^{-\lambda(t-T)} & \text{for } t > T \end{cases} \quad (6a)$$

$$m_{Out}(t) = m_0 - m_S(t) + \begin{cases} \Phi t & \text{for } t \leq T \\ \Delta\Phi T + \phi_0 t & \text{for } t > T \end{cases} \quad (6b)$$

where $\Delta\Phi = \Phi - \phi_0$. The dashed lines in Fig. 4*A* show that m_S increases to a steady state for $t < T$, followed by an exponential decrease back to the baseline value for $t > T$. Similarly, Fig. 4*B* shows that m_{Out} increases at a greater rate than Φ increases for $t < T$, subsequently becoming parallel to the baseline curve for $t > T$. The critical current Φ^* for which jamming occurs can be evaluated by requiring that $m_S(T) = m_P$ for $\Phi = \Phi^*$, which gives $\Phi^* = \lambda\,(m_P - m_0 e^{-\lambda T})/(1 - e^{-\lambda T})$. Since $m_0 < m_P$, the critical current $\Phi^* > Q_{max}$. For long stretching periods, $T >> 1/\lambda$, $\Phi^* \rightarrow Q_{max}$. The thick solid line in Fig. 4*B* shows that $m_{Out}(t)$ is the largest in this case for $t > T$.

For $\Phi > \Phi^*$, the dynamics of surfactant release can be divided into four distinct phases. Since the outflow $Q(t) < \Phi$, m_S increases from m_0 at $t = 0$. We define $T_1 < T$ as the time of onset of jamming such that $m_S(T_1) = m_P$. Thus, for $0 \leq t \leq T_1$, the solutions of *Eq. 3* are

$$m_S(t) = \left(m_0 - \frac{\Phi}{\lambda}\right)e^{-\lambda t} + \frac{\Phi}{\lambda} \quad (7a)$$

$$m_{Out}(t) = \left(m_0 - \frac{\Phi}{\lambda}\right)\left(1 - e^{-\lambda t}\right) + \Phi t \quad (7b)$$

Solving $m_S(T_1) = m_P$ in *Eq. 7a* gives $T_1 = \lambda^{-1} \log [(\Phi - \lambda\, m_0)/(\Phi - Q_{max})]$.

For $T_1 < t \leq T$, the system is jammed, while $\phi(t) = \Phi$ continues to drive m_S toward M. In this phase, the solutions to *Eq. 3* yields

$$m_S(t) = M - (M - m_P)e^{-\lambda_1(t-T_1)} \quad (8a)$$

$$m_{Out}(t) = m_{Out}(T_1) + \frac{Q_{max}}{\lambda_1}\left[1 - e^{-\lambda_1(t-T_1)}\right] \quad (8b)$$

where $\lambda_1 = (\Phi - Q_{max})/(M - m_P)$ provides a second time constant.

For $t > T$, stretching ceases, the current $\phi(t) = \phi_0$, and, although the system is jammed, m_S begins to decrease. We define T_2 as the time when the jamming ends, such that $m_S(T_2) = m_P$. Thus, for $T < t \leq T_2$, the solution of *Eq. 3* is

$$m_S(t) = M - (M - m_P)e^{-\lambda_2(T_2 - t)} \quad (9a)$$

$$m_{Out}(t) = m_{Out}(T) + \frac{Q_{max}}{\lambda_2}\left[e^{-\lambda_2(T_2-T)} - e^{-\lambda_2(T_2-t)}\right] \quad (9b)$$

where $\lambda_2 = (Q_{max} - \phi_0)/(M - m_P)$. The time T_2 can be calculated as the point when jamming ends, $m_S(T_2) = m_P$, giving $T_2 = (1 + \lambda_1/\lambda_2)\,T - (\lambda_1/\lambda_2)\,T_1$. The time constants $1/\lambda_1$ and $1/\lambda_2$ provide the time scales for increasing and decreasing surface mass in the jammed state.

Finally, for $t > T_2$, the system gets out of the jammed state, and the solutions can be written as

$$m_S(t) = \left(m_P - \frac{\phi_0}{\lambda}\right)e^{-\lambda(t-T_2)} + \frac{\phi_0}{\lambda} \quad (10a)$$

$$m_{Out}(t) = m_{Out}(T_2) + \left(m_P - \frac{\phi_0}{\lambda}\right)\left[1 - e^{-\lambda(t-T_2)}\right] + \phi_0(t - T_2) \quad (10b)$$

The dashed lines in Fig. 5 show the dynamics of m_S and m_{Out} for $\Phi > \Phi^*$. With increasing Φ, $m_S \rightarrow M$ during the stretching phase $t \leq T$ and takes increasingly longer times to recover from jamming after stretching stops. The secreted mass m_{Out} shows a characteristic flat region during the jammed phase and quickly increases after jamming ceases.

The above expressions for $m_{Out}(t)$ allow us to fit the experimental data in Fig. 2 to obtain model parameters m_0, λ, M, ϕ_0, and Φ. We note that, since all parameters contain m_P as a multiplicative factor, the value of m_P cannot be obtained from the fitting procedures. First, m_0, λ, and ϕ_0 are obtained by fitting the unstretched data (Fig. 2, circles) using *Eq. 4* and assuming that no jamming occurs in the unstretched case. Next, the same parameters are used for the curves corresponding to $T = 15$, 30, and 60 min (Fig. 2, squares, diamonds, and triangles) to obtain fitted values for M and Φ. Figure 2 shows the fitted curves thus obtained (solid lines).

To relax the assumption that our model consists of identical cells releasing surfactant in response to identical stretch, we numerically investigated the separate effects of *1*) heterogeneous distribution of stretch in the system, and *2*) heterogeneous cell sizes. To investigate the effect of a heterogeneous stretch distribution, we assume that stretch is directly related to Φ, and thus we assign distinct values of Φ_i for each cell i

$$\Phi_i = (1 + \xi_i)\langle\Phi\rangle \quad (11)$$

where ξ_i are time-independent random numbers drawn from a uniform distribution with zero mean and standard deviation $\sigma_1 < 1$, and the operator $<\ldots>$ represents the average over a large sample of the appropriate random variable. Similarly, when cell sizes are heterogeneous, we assume that the parameters m_P, M, and Q_{max} are directly proportional to cell size. Thus we assign a different value of these parameters for each cell i

$$m_{P,i} = (1 + \eta_i)\langle m_P\rangle \quad (12a)$$

$$M_i = (1 + \eta_i)\langle M\rangle \quad (12b)$$

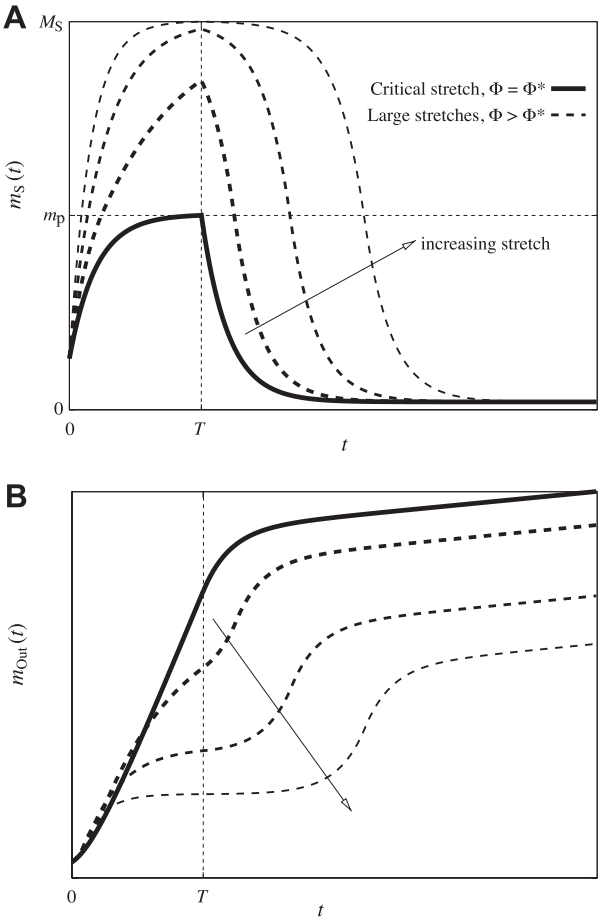

Fig. 5. Model results for the mass of surfactant in arbitrary units at the surface $m_S(t)$ (*A*) and in the extracellular space $m_{Out}(t)$ (*B*) for *1*) critical stretch, which initiates jamming, $\Phi = \Phi^*$, shown as solid line; and *2*) large stretches, which cause jamming, $\Phi > \Phi^*$, described by *Eqs. 7–10*, shown as dashed lines. Arrows indicate increasing Φ.

$$Q_{max,i} = (1 + \eta_i)\langle Q_{max}\rangle \qquad (12c)$$

where η_i are time-independent random numbers that are distributed uniformly with zero mean and standard deviation $\sigma_2 < 1$. The values of $<\Phi>$, $<m_P>$, $<M>$, and $<Q_{max}>$ are identical to the ones obtained from the model fits, such that, in the limit $\sigma \rightarrow 0$, the heterogeneous model reproduces the homogeneous one. Since our model ignores cell-cell interactions, the normalized secretion of a population of cells is identical to the average of the secretion by individual cells. We thus solve *Eq. 3* for each cell and compute $<m_S(t)>$ and $<m_{Out}(t)>$.

Figure 6 shows the effects of simulated heterogeneity on the secretion dynamics for cells stretched up to $T = 15$ min. The parameters m_0, λ, and ϕ_0, as well as the mean values $<\Phi>$, $<m_P>$, $<M>$, and $<Q_{max}>$ were identical to those obtained from the model fits in Fig. 2. In the absence of heterogeneity, $\sigma_1 = 0$ and $\sigma_2 = 0$, the time course of secreted surfactant outside the cell $<m_{Out}>$ as shown by solid lines in Fig. 6, *B* and *D*, are identical to the fitted results obtained for $T = 15$ min (dash-dotted lines in Fig. 2). With increasing heterogeneity in stretch amplitude (Fig. 6, *A* and *B*), as well as cell size (Fig. 6, *C* and *D*), the release of the jammed surfactant stored at the surface starts earlier, while, at the same time, it takes longer to completely release the excess surfactant. This results in a less pronounced shoulder in $<m_S>$ or knee in $<m_{Out}>$. However, the general shape of the surfactant secretion curves remains the same.

DISCUSSION

Secretory processes by various cells are studied either at the level of a population of cells using molecular biology (27) or at the level of individual surfactant molecules passing through fusion-pores using biophysical methods (16). While it is possible to visualize individual LBs, one would need an enormous number of observations at the microscopic level to average out the fluctuations of individual molecules passing through the fusion pores. In this study, we used radioactive labeling and directly measured the bulk secreted surfactant from tens of thousands of cells, which allows us to observe and quantify the stretch-induced dynamics of surfactant secretion by AEII cells already in a smooth and averaged fashion. Specifically, using this approach, we found that the secretion of surfactant by AEII cells exhibits a collective behavior at the level of single cells.

The experimental observations in this study are in qualitative agreement with previous results, which indicated that a significant increase in extracellular surfactant was only observed long after the stretch stopped (12, 27). Our data not only quantify this delayed increase in stretch-induced secretion, but also demonstrate that large-amplitude cyclic stretch serves to inhibit surfactant secretion in AEII cells during and immediately after the stretching phase.

In selected groups, Western blot analysis of surfactant protein B, which is packed and secreted together with PC, demonstrated similar results to the lipids (2). This indicated that the measured radioactivity was of surfactant rather than cell membrane origin. Cells with damaged membranes, which were subsequently repaired by the 60-min time point, would also cause an increase in extracellular PC without indicating the damage during the live-to-dead ratio test. We note, however, that, if plasma membrane damage was a significant contributor to the increased PC secretion, this would also enhance the secretion during the longer term stretching protocols (30 and 60 min). In addition, the fraction of dead cells did not significantly change with time of stretch, which indicates that the released surfactant was a result of a cellular secretion rather than due to cell injury or death.

We modeled the secretion of surfactant from AEII cells to explain two key aspects of the experimental results: *1*) during and immediately after stretch, cells secreted less surfactant than unstretched cells; and *2*) cells stretched for 15 min secreted significantly more surfactant than unstretched cells after ~45 min of rest. The former indicates that stretching suppressed surfactant secretion, while the latter implies that the system retained a memory of the stretch. The subsequent increase in secretion suggests that stretch indeed induces an enhancement of surfactant secretion, but the delay implies that the rate of secretion is in fact decreased.

In general, the release of surfactant from the cell would involve a sequence of steps, such as packaging the surfactant into LBs, transport of the LBs to the cell membrane, fusion of the LBs to the membrane to form a fusion pore, and opening of the fusion pore to release the surfactant (9). Each step in such a sequence would be dependent on the predecessors, and the

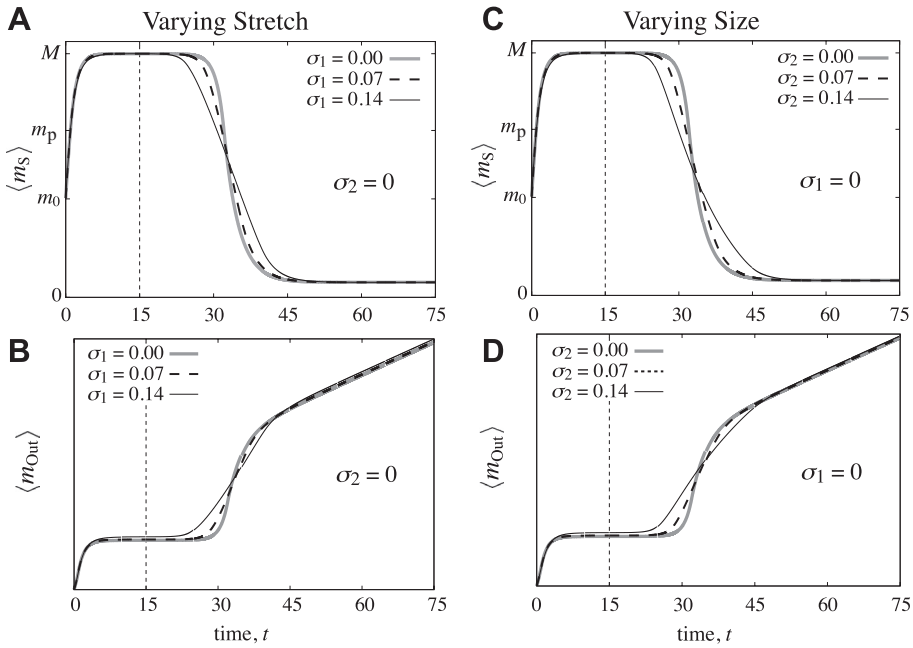

Fig. 6. Model results, in arbitrary units, showing the changes in surfactant secretion due to variability in stretch (*A* and *B*) and size (*C* and *D*) for cells stretched for $T = 15$ min using the fitted parameters from Fig. 2. *A* and *C* show the normalized mass of surfactant on the surface $<m_S>$, whereas *B* and *D* show the normalized mass of surfactant on the outside the cell $<m_{Out}>$ for simulations corresponding to no variability ($\sigma_{1,2} = 0$, thick gray lines), as well as for $\sigma_{1,2} = 0.07$ (dashed lines), and $\sigma_{1,2} = 0.14$ (thin solid lines).

dynamics of the process would depend on the dynamics of each individual step, as well as the stretch-induced changes of each step. However, this process is simplified if one of these steps is much slower than the others, where the slow step or bottleneck becomes the dominant step of the dynamics. In this case, all other processes are virtually instantaneous, and the overall dynamics of surfactant release can then be well approximated by the dynamics of the bottleneck step, regardless of the location of the bottleneck in the sequence. Moreover, the stretch response of the bottleneck becomes the only relevant determinant to the stretch response of surfactant release. Thus we restrict our modeling to a single equivalent "surface" compartment, which represents the slowest process in the surfactant secretory dynamics.

To better understand this bottleneck phenomenon, we examine a simple linear secretion process. Figure 7*A* shows a simple linear model described by the equations

$$\frac{dm_s}{dt} = \phi - km_S \quad (13a)$$

$$\frac{dm_{Out}}{dt} = Q = km_S \quad (13b)$$

where the rate k and input flow ϕ could depend on the stretch. We assume that, during stretch, $0 \le t \le T$, $k \to k^*$, and $\phi \to \Phi$. Notice that, in the absence of stretch, $t > T$, $k \to k_0$, and $\phi \to \phi_0$. First, we note that, if the input flow ϕ is independent of stretch, that is $\Phi = \phi_0$, the mass of secreted surfactant, m_{Out}, would converge to that for the unstretched case after sufficient time has elapsed after the stretch. Thus the long-term amount of released surfactant cannot increase beyond that during the spontaneous release, if stretch only affects the rate constant k.

To mimic the experimental result, where m_{Out} increases at a slower rate during stretch, we can assume that k decreases during stretch, $k^* < k_0$. At the same time, since m_{Out} increases beyond the unstretched case after sufficient time, ϕ must increase with stretch, $\Phi > \phi_0$. A salient property of a bottleneck is the formation of a reservoir of mass m_S upstream the bottleneck, which can be controlled by k. During stretch, m_S increases as a result of increased inflow Φ, as well as decreased outflow $k\ m_S$. Once the stretch stops, this excess mass in the reservoir is released, and m_{Out} increases. Figure 7*B* shows the dynamics of surfactant release from this simple linear model. We note that, using this model, we could match the unstretched case (solid curve), as well as the 15-min and 60-min time points when $T = 15$ min. However, the model is unable to match the 30-min time point for $T = 15$ min, as well as all the independent points for $T = 30$ min and 60 min. To estimate the quality of the fits, we calculated the root-mean-squared relative error for the linear model, as well as our jamming model for all data points and their corresponding model fits. The root-mean-squared relative error for the linear model was 40%, while that of the jamming model was 17%. The reason for this is that a

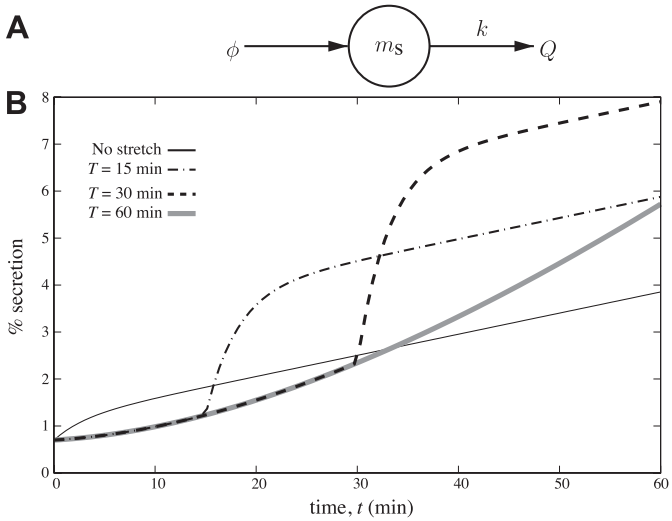

Fig. 7. Illustration (*A*) and dynamics (*B*) of a simple linear model of surfactant secretion.

single rate constant, k_0, governs the release of surfactant from the reservoir. This rate is independent of the reservoir mass m_S. We conclude that the dynamics of the secretion of surfactant is a fundamentally nonlinear process with memory.

The inability of the above general linear model to account for these dynamic features leads us to invoke a jamming model inspired by observed phenomena in the dynamics of vehicular traffic, escape panic, and related systems (7, 8, 18, 19). Simply, we hypothesized that stretch induces an increased current of surfactant from the interior of the cell to the exterior. However, this transport is mediated by a surface layer in the cell, which has a finite capacity due to the limited number of fusion pores. When the amount of surfactant in the surface layer approaches this capacity, there will be interference among LBs carrying the surfactant, and this interference causes a decrease in the amount of secreted surfactant per unit time and hence effectively creating a jam. When stretch stops, the jam takes an extended time to clear, and subsequently the amount of secreted surfactant increases. This process, therefore, also produces memory of the system.

We also note that, for small increases in the input flow, $\Phi < \Phi^*$, the jamming model behaves like the simple linear model and no jamming occurs. However, once $\Phi > \Phi^*$, the surface mass m_S eventually exceeds the threshold m_P, and the system enters a jammed phase, and the relation between outflow Q and m_S reverses such that increased m_S leads to decreased outflow. Once the stretch stops, the system remains in the jammed phase while $m_S > m_P$. The characteristic time $T_2 - T$ to recover from the jam after stretch ceases is proportional to the length of time $T - T_1$ spent in the jammed phase during stretch, unlike the constant recovery time for the simple linear process. Thus this model is able to capture the salient features of the dynamics of surfactant secretion by AEII cells, including its temporary inhibition and the subsequent enhancement due to cyclic stretch (Fig. 2).

The model also provides several testable predictions. In the jammed state, the mass m_S should increase, which could be directly observed following different stretch patterns. Although stretching for longer than 15 min does not show enhanced secretion within 1 h, our model suggests that such an increase should be observable at even longer times, unless other intracellular processes break down the activated but jammed LBs.

While the simplicity of the model allows analytic solutions, it is also accompanied by several limitations. First, we modeled the cell population by the dynamics of a single representative cell. This mean field approach neglects the difference in the response of individual cells, as well as their known interaction (9). We thus numerically explored the effect of heterogeneous cell sizes and the effect of nonuniform stretch. In both cases, the time course of surfactant secretion remains qualitatively similar, although the secretion process starts somewhat earlier and ends later after the cessation of stretch. This is due to the fact that larger cells or cells experiencing smaller stretches are less jammed than smaller cells or cells experiencing larger stretches. Cells that are less jammed can clear their excess surfactant quicker than cells that are more jammed. It is also worth noting that the effects of heterogeneous cell size and heterogeneous cell stretch on secretion dynamics are similar (Fig. 6), and hence it is unlikely that they could be experimentally resolved by simply observing bulk secretion.

In addition, we do not account for the uptake of the secreted surfactant, assuming that its low extracellular concentration (<10%) has a negligible effect on the dynamics. This is reasonable given that, in the present study, as well as in our recent experimental study, we found little effect of stretch on surfactant uptake, as shown in Table 2 (3). Our model also does not explicitly account for the physical or chemical interaction among LBs, but such interference is implicitly taken into account as a jamming process. It is known that various chemical substances stimulate surfactant secretion (23). While the effect of stretch was incorporated into $\phi(t)$ by increasing it from ϕ_0 to Φ, we can also think of the change in $\phi(t)$ as a result of chemical stimulation. Therefore, it is possible that jamming would occur during chemical stimulation. Indeed, in neuronal cells, synaptic endocytosis was shown to be severely impaired after strong stimulation (13), which was interpreted as traffic jams at synapses (26). In AEII cells, a similar mechanism may take place. Visual inspection of Fig. 1*A* in the study by Frick et al. (14) reveals clusters of stimulated LBs just under the cell membrane after stimulation with ATP. Additionally, cell-cell interactions, either mechanical or through signaling that can modify the secretion, is not considered in the model. However, it is thought that type I epithelial cell signaling plays an important role in the secretory response of AEII in vivo (20). Finally, the biophysical and biochemical properties of the underlying substrate may also influence secretion (4). Thus the applicability of our results may be limited to the pure AEII cell culture, and this issue warrants further experimental verification.

The piecewise-linear fundamental diagram with a single peak (Fig. 3) describes the average jamming behavior of LBs and does not specify the mechanism that leads to jamming. Fusion pores, through which the surfactant is released from the LBs, are dynamic, rate-limiting structures (16), and hence their ability to stay open could be hampered by the presence of large queues of LBs. Regulated surfactant secretion through fusion pores requires specific membrane-bound target SNARE (soluble *N*-ethylmaleimide-sensitive factor attachment protein receptors) proteins called SNAP-23 and syntaxin-2 (1). Recently, it was shown that syntaxin molecules in the plasma membrane naturally self-organize into clusters due to a weak attractive interaction between the molecules, but the size of the clusters is limited by crowding-induced repulsion (24). We speculate that this mechanism organizes the available syntaxin in the membrane into a finite-number docking sites, allowing jamming to occur when secretion is strongly stimulated. Stretch could directly influence these docking protein clusters together with the fusion pore opening dynamics. Stretching is known to affect the openings of calcium channels that are required for secretion (27). At high concentrations, LBs could also form large aggregates, which would take a longer time to empty through the fusion pores. Thus, although jamming provides a simple unified mechanism to explain the delayed enhancement of secretion in response to stretch, alternate models involving more specific time-dependent responses of the various subsystems of the secretory pathway could also lead to similar results.

Despite the above limitations, our model captures the key features of the dynamics of surfactant secretion observed under the current experimental conditions. The proposed mechanism of jamming highlights the importance of dynamics in cellular secretory response to applied stretch. In several diseases, such

as respiratory distress syndrome in premature infants (25), where the surfactant pool is not sufficient to maintain a physiologically appropriate low level of surface tension in the alveoli, it is often desirable to quickly replenish the surfactant pool, which has either been depleted or rendered ineffective (17). Additional experiments mapping the effects of both timing and amplitude of stretch could make it possible to tune stretch patterns for avoiding the jammed state and hence maximizing surfactant release. It is possible that jamming is avoided during variable stretch patterns that have been reported to increase surfactant release (3). Finally, jamming could also be relevant to the dynamics of stimulated secretion by other means, as well as by other cells in vivo, such as cells in the vascular or endocrine systems.

GRANTS

This study was supported by National Heart, Lung, and Blood Institute (HL-098976).

DISCLOSURES

No conflicts of interest, financial or otherwise, are declared by the author(s).

AUTHOR CONTRIBUTIONS

Author contributions: A.M., S.P.A., E.B.-S., and B.S. conception and design of research; A.M., S.P.A., and H.P. analyzed data; A.M., E.B.-S., and B.S. interpreted results of experiments; A.M. prepared figures; A.M. drafted manuscript; A.M., E.B.-S., and B.S. edited and revised manuscript; A.M., S.P.A., E.B.-S., H.P., and B.S. approved final version of manuscript; S.P.A., E.B.-S., and B.S. performed experiments.

REFERENCES

1. **Abonyo BO, Gou D, Wang P, Narasaraju T, Wang Z, Liu L.** Syntaxin 2 and SNAP-23 are required for regulated surfactant secretion. *Biochemistry* 43: 3499–3506, 2004.
2. **Arold SP.** *Effects of Cyclic Stretch on Surfactant Secretion and Cell Viability in Alveolar Epithelial Cells Grown in Culture* (PhD thesis). Boston, MA: Boston University, 2006.
3. **Arold SP, Bartolak-Suki E, Suki B.** Variable stretch pattern enhances surfactant secretion in alveolar type II cells in culture. *Am J Physiol Lung Cell Mol Physiol* 296: L574–L581, 2009.
4. **Arold SP, Wong JY, Suki B.** Design of a new stretching apparatus and the effects of cyclic strain and substratum on mouse lung epithelial-12 cells. *Ann Biomed Eng* 35: 1156–1164, 2007.
5. **Bachofen H, Schurch S.** Alveolar surface forces and lung architecture. *Comp Biochem Physiol A Mol Integr Physiol* 129: 183–193, 2001.
6. **Burgess TL, Kelly RB.** Constitutive and regulated secretion of proteins. *Annu Rev Cell Biol* 3: 243–293, 1987.
7. **Chowdhury D, Santen L, Schadschneider A.** Statistical physics of vehicular traffic and some related systems. *Phys Rep* 329: 199–329, 2000.
8. **Chowdhury D, Schadschneider A, Nishinari K.** Physics of transport and traffic phenomena in biology: from molecular motors and cells to organisms. *Phys Life Rev* 2: 318–352, 2005.
9. **Dietl P, Haller T.** Exocytosis of lung surfactant: from the secretory vesicle to the air-liquid interface. *Annu Rev Physiol* 67: 595–621, 2005.
10. **Ding J, Warriner HE, Zasadzinski JA.** Viscosity of two-dimensional suspensions. *Phys Rev Lett* 88: 168102, 2002.
11. **Dobbs LG.** Isolation and culture of alveolar type II cells. *Am J Physiol Lung Cell Mol Physiol* 258: L134–L147, 1990.
12. **Edwards YS.** Stretch stimulation: its effects on alveolar type II cell function in the lung. *Comp Biochem Physiol A Mol Integr Physiol* 129: 245–260, 2001.
13. **Ferguson SM, Brasnjo G, Hayashi M, Wölfel M, Collesi C, Giovedi S, Raimondi A, Gong LW, Ariel P, Paradise S, O'Toole E, Flavell R, Cremona O, Miesenböck G, Ryan TA, De Camilli P.** A selective activity-dependent requirement for dynamin 1 in synaptic vesicle endocytosis. *Science* 316: 570–574, 2007.
14. **Frick M, Eschertzhuber S, Haller T, Mair N, Dietl P.** Secretion in alveolar type II cells at the interface of constitutive and regulated exocytosis. *Am J Respir Cell Mol Biol* 25: 306–315, 2001.
15. **Haller T, Ortmayr J, Friedrich F, Volkl H, Dietl P.** Dynamics of surfactant release in alveolar type II cells. *Proc Natl Acad Sci USA* 95: 1579–1584, 1998.
16. **Haller T, Pfaller K, Dietl P.** The conception of fusion pores as rate-limiting structures for surfactant secretion. *Comp Biochem Physiol A Mol Integr Physiol* 129: 227–231, 2001.
17. **Hamm H, Kroegel C, Hohlfeld J.** Surfactant: a review of its functions and relevance in adult respiratory disorders. *Respir Med* 90: 251–270, 1996.
18. **Helbing D.** Traffic and related self-driven many-particle systems. *Rev Mod Phys* 73: 1067–1141, 2001.
19. **Helbing D, Farkas I, Vicsek T.** Simulating dynamical features of escape panic. *Nature* 407: 487–490, 2000.
20. **Isakson BE, Seedorf GJ, Lubman RL, Evans WH, Boitano S.** Cell-cell communication in heterocellular cultures of alveolar epithelial cells. *Am J Respir Cell Mol Biol* 29: 552–561, 2003.
21. **Lehmann H.** Distribution function properties and the fundamental diagram in kinetic traffic flow theory. *Phys Rev E Stat Phys Plasmas Fluids Relat Interdiscip Topics* 54: 6058–6064, 1996.
22. **Prank K, Kloppstech M, Nowlan SJ, Sejnowski TJ, Brabant G.** Random secretion of growth hormone in humans. *Phys Rev Lett* 77: 1909–1911, 1996.
23. **Rooney SA.** Regulation of surfactant secretion. In: *Lung Surfactant: Cellular and Molecular Processing*, edited by Rooney SA. Austin, TX: Landes, 1998.
24. **Sieber JJ, Willig KI, Kutzner C, Gerding-Reimers C, Harke B, Donnert G, Rammner B, Eggeling C, Hell SW, Grubmüller H, Lang T.** Anatomy and dynamics of a supramolecular membrane protein cluster. *Science* 317: 1072–1076, 2007.
25. **Verma RP.** Respiratory distress syndrome of the newborn infant. *Obstet Gynecol Surv* 50: 542–555, 1995.
26. **Wiedemann C.** Vesicular trafficking: traffic jam at the synapse. *Nat Rev Neurosci* 8: 405, 2007.
27. **Wirtz HR, Dobbs LG.** Calcium mobilization and exocytosis after one mechanical stretch of lung epithelial cells. *Science* 250: 1266–1269, 1990.